

10-2016

## A Smartphone Compatible SONAR Ranging Attachment for 2-D Mapping

Daniel Graham

*William & Mary*, [dggraham@cs.wm.edu](mailto:dggraham@cs.wm.edu)

Gang Zhou

*William & Mary*, [gzhou@cs.wm.edu](mailto:gzhou@cs.wm.edu)

Ed Novak

*William & Mary*, [ejnovak@email.wm.edu](mailto:ejnovak@email.wm.edu)

Jeffrey Buffkin

*William & Mary*

Follow this and additional works at: <https://scholarworks.wm.edu/aspubs>

---

### Recommended Citation

Graham, Daniel; Zhou, Gang; Novak, Ed; and Buffkin, Jeffrey, A Smartphone Compatible SONAR Ranging Attachment for 2-D Mapping (2016). *IEEE INTERNET OF THINGS JOURNAL*, 3(5).  
10.1109/JIOT.2015.2502486

This Article is brought to you for free and open access by the Arts and Sciences at W&M ScholarWorks. It has been accepted for inclusion in Arts & Sciences Articles by an authorized administrator of W&M ScholarWorks. For more information, please contact [scholarworks@wm.edu](mailto:scholarworks@wm.edu).

# A Smartphone Compatible SONAR Ranging Attachment for 2-D Mapping

Daniel Graham, Gang Zhou, Ed Novak, and Jeffrey Buffkin

**Abstract**—The ability to attach external devices to smartphones has revolutionized the role of smartphones by extending their capabilities beyond the limitations of commodity hardware. Developing external attachments that allow smartphones to sense the depth of an area will facilitate the development of new immersive applications and technologies. In this paper, we propose a smartphone compatible SONAR ranging attachment and address the compatibility problem by proposing a hybrid hardware/software modulator that allows a digital sensor to communicate with a smartphone via the 3.5-mm headphone jack, found on most smartphones. We evaluate the proposed sensor using two metrics, accuracy and spatial resolution. We evaluate the accuracy of this system by measuring known distances with the sensor and comparing them. We measure the sensor’s spatial resolution by using ranging information from the SONAR module along with the phone’s gyroscope, accelerometer, and magnetometer to construct a two-dimensional map of a space.

**Index Terms**—Smartphones, SONAR.

## I. INTRODUCTION

SMARTPHONES have allowed companies to replace custom embedded solutions with more cost-effective smartphone attachments. For example, Honeywell’s point-of-sale (POS) attachment has allowed vendors to replace expensive, custom handhelds with standard smartphones and relatively cheap hardware attachments [1]. Recently, there has been emerging interest in developing attachments that provide depth sensing capabilities. Allowing smartphones to sense depth opens mobile computing research to a variety of interesting possibilities.

In this paper, we attempt to solve the problem of providing depth sensing capabilities to smartphones by designing an external SONAR attachment. Ideally, we would like to leverage existing research by using in-air SONAR modules from the area of robotics. However, there are currently no hardware or software interfaces that allow us to connect existing sensors to a smartphone. Thus, in an effort to leverage existing sonar modules, we have designed a hardware and software interface that allows us to connect an existing SONAR sensor (like the LV-MaxSonar-EZ 1), to a smartphone. Fig. 1 shows a photograph of our hardware interface with the sensor attached.

Currently, there are three possible approaches for connecting an external attachment to a smartphone: bluetooth, the micro-USB port, and the headphone jack. Connecting the attachment

Manuscript received October 01, 2015; accepted November 12, 2015. Date of publication November 19, 2015; date of current version September 08, 2016. This work was supported by the U.S. National Science Foundation under Grant CNS-1250180 and Grant CNS-1253506 (CAREER).

The authors are with the Department of Computer Science, College of William and Mary, Williamsburg, VA 23185 USA (e-mail: dggraham@cs.wm.edu).

Digital Object Identifier 10.1109/IIOT.2015.2502486

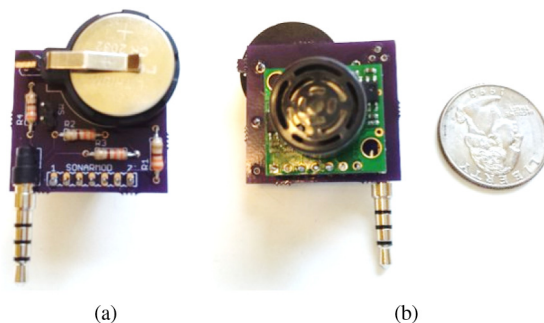


Fig. 1. (a) Photograph of the 3.3-V battery, the modulator circuit, and the male 3.5-mm male headphone jack adapter. (b) Photograph of the transducer module.

using a bluetooth connection allows the attachment to remain physically untethered from the smartphone but increases the energy consumption and cost of the attachment. Connecting the attachment using a USB connection allows the external attachment to be powered by the smartphone. However, since not all modern phones directly support the USB standard (e.g., the Apple iPhone), these USB attachments will only be compatible with a subset of attachments.

Current systems which utilize the headphone jack have been designed to interface with external modules by simply reading analog values from the sensor. However, if the sensor produces a logic level signal, the analog-to-digital converter (ADC) on a typical smartphone is unsuited from reading the signal. This presents a challenge, since the SONAR sensor we use is a digital sensor, and therefore encodes its information using logic level signals [2]. We address the smartphone’s limitations by proposing a hybrid hardware/software modulator that converts these logic level signals into modulated continuous wave (MCW) signals, which are similar to the modulation strategy that was used by Samuel Morse when he developed Morse code telegraphy [12]. These signals can be read by the smartphone. When thinking about how MCW modulation works in the proposed context, it is important to consider the symbol space. Morse code has a symbol space of size two: a long beep and a short beep. Intuitively, it is possible to think of the proposed scheme as having a symbol space of  $n$ , where  $n$  represents the resolution with which the pulse is measured. Our proposed modulator is a key component in the design of our external attachment, since it is what makes communication between the attachment and the phone possible.

Our external SONAR attachment is comprised of an ultrasonic transducer, a microcontroller, a modulator, and a standard “coin cell” battery. The ultrasonic transducer is responsible for generating the ultrasonic signal, which travels through the air

until it is reflected by a nearby surface. The reflected wave is then captured by the transducer. Once the signal has been captured, the microcontroller calculates the distance to the object by examining the time delay between the initial signal and its reflection. Once the distance has been determined, the microcontroller generates a pulse-width modulated signal whose length is directly related to the measured distance. This signal is then fed to the modulator, which converts the pulse-width modulated signal into an MCW signal, which is sent to the smart device through the headphone jack. The device can read these signals and decodes them, in software, to receive the distance information. Once the distance is decoded, the next step is to determine the direction of the received wave. This is done using the phone's gyroscope, accelerometer, and magnetometer to determine the phone's current orientation. By taking a collection of repeated measurements, it is possible to construct a simple 2-D map of the space.

In this paper, we make the following contributions.

- 1) We design and build an in-air SONAR module that can be paired with commodity smartphones.
- 2) We propose the use of a hybrid hardware/software modulator for communicating between the external module and the smartphone, via a standard 3.5-mm headphone jack.
- 3) We propose, implement, and evaluate a linear time algorithm for demodulating the MCW signal.
- 4) We build a prototype of our system and evaluate its performance, showing precision on the order of inches.
- 5) We propose and implement an approach for combining the range and directional information to generate a 2-D map of a space.

## II. DESIGN

The system is comprised of three major components: 1) an external SONAR module; 2) a commodity smartphone; and 3) the software application running on the phone. Fig. 2 shows a diagram of the system's architecture. The external SONAR module is designed to use a collection of ultrasonic chirps to measure the distance to an object. Once the distance has been measured, the external module generates a modulated analog signal with the encoded information, and transmits it to the phone's hardware, through the headphone jack. The smartphone receives the signal and converts it to a digital vector using its own, on-board ADC. In addition to sampling and converting the signal, the smartphone is also responsible for tracking the phone's orientation and, by extension, the attachment's orientation, using its own internal gyroscope, accelerometer, and magnetometer. The range and direction information is then combined by a software application to generate a direction vector. This vector represents the distance and direction of the item or surface, which reflected the original ultrasonic signal. These distance vectors can then be combined to generate a 2-D map of a space.

### A. External Attachment

There are currently no commercial off-the-shelf (COTS) interfaces that allow us to connect a SONAR

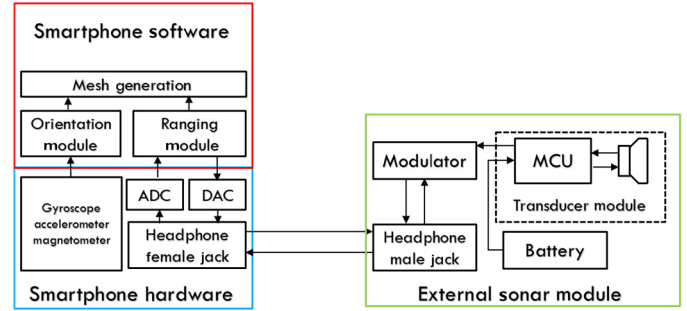


Fig. 2. System diagram of the proposed SONAR system, which is comprised of: 1) an external SONAR module, 2) a commodity smartphone, and 3) the software application running on the phone.

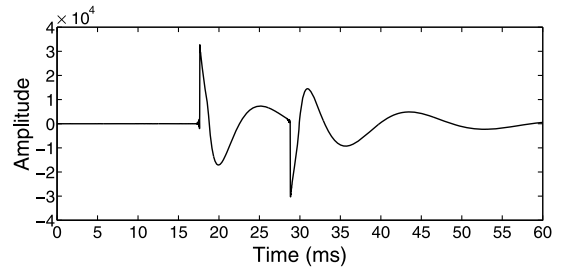


Fig. 3. Signal that is reconstructed when the pulse-width modulated signal is fed directly to the phone.

sensor to a smartphone. Since there are no existing interfaces or drivers, we have designed and built a headphone jack interface and designed an MCW modulation scheme that allows us to connect an existing SONAR module to a smartphone. In this section, we describe the hardware that comprises the headphone jack interface, and the SONAR transducer module.

The external module hardware (shown in Fig. 1) is comprised of three major components: a transducer module (the LV-MaxSonar-Ez 1), a modulator circuit, and a 3.5-mm male headphone jack adapter [2]. The transducer module contains a microcontroller and an ultrasonic transducer. The transducer module is responsible for generating the ultrasonic chirps, and calculating the distance of the object by measuring the elapsed time between the chirps. This distance is encoded as a pulse-width modulated signal where each  $147\mu\text{s}$  represents 1 inch. This signal is a logic level signal, and it cannot be decoded by the phone if it is directly fed to the phone's headphone jack. Fig. 3 shows the signal that is decoded by the phone's ADC when the pulse width modulated signal is fed directly to the phone. Notice that it is difficult to determine the width of the pulse. We suspect that this poor reconstruction may be due to the fact that the phone's ADC is preceded by ac coupling. However, we cannot confirm this because the phone's hardware is proprietary.

The modulator is responsible for transforming the pulse-width modulated signals from the transducer module into an ac signal that the phone can decode. This is done by designing a circuit that generates an MCW from the pulse-width modulated signal. The MCW is then fed to the phone via its headphone jack.

1) *Modulator*: The modulator takes two inputs, a carrier and the pulse-width modulated signal, and produces an MCW.

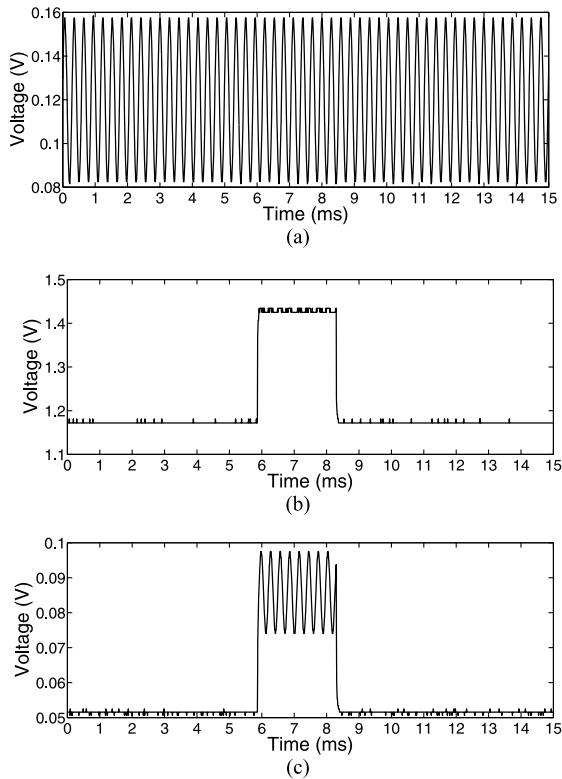


Fig. 4. (a) 3804-kHz carrier frequency that is generated on the phone. (b) Pulse-width modulated signal that is generated by the transducer module. (c) MCW signal that encodes the distance information. These measurements were taken using an object that was 43 cm away from the sensor.

It is possible to generate the carrier using a hardware oscillator, such as a crystal oscillator, which uses the mechanical vibrations of a piezoelectric crystal to generate a periodic signal. Crystal oscillators are commonly used in radios to generate the carrier frequency [10]. However, including this hardware increases the size and cost of the platform. Instead, we implement the oscillator in software by leveraging the functionality of the phone’s digital-to-analog converter (DAC) to generate the carrier. Once the carrier has been generated, it is fed to the modulator through the headphone jack. Fig. 4 shows the signals that are involved in the modulation process.

It is important to select the correct frequency for the carrier. Selecting a carrier frequency that is too high may prevent the ADC from converting the signal, since the ADC may not support the sampling rate that is required. Selecting a carrier frequency that is too low may not provide enough resolution to accurately decode the length of the signal. The datasheet of the transducer module indicates that the pulse-width modulated signal has a resolution of  $147\ \mu\text{s}$ , where each  $147\ \mu\text{s}$  corresponds to 1 in [2]. Ideally, we would like to design the carrier so that each peak in the carrier corresponds to a single inch as well. This means that we would need to create a 6.8-kHz carrier. However, the frequency of this carrier is too high for the ADC on the phone to accurately recover the peaks in the signal. To mitigate this, we selected a frequency of 3.4 kHz. This is half the original, which means each peak corresponds to 2 inches. However, it is possible to get a resolution of an inch at this frequency by also counting troughs, since each trough represents half the distance between two peaks.

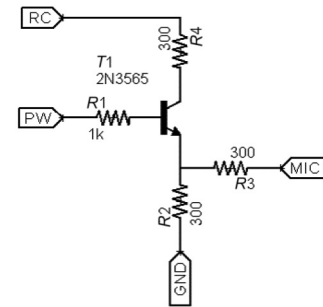


Fig. 5. Circuit schematic of the modulation circuit. RC is the label for the received carrier. PW is the label for the pulse-width modulated signal. MIC is the label for the output of the modulator that is connected to the microphone input on the phone.

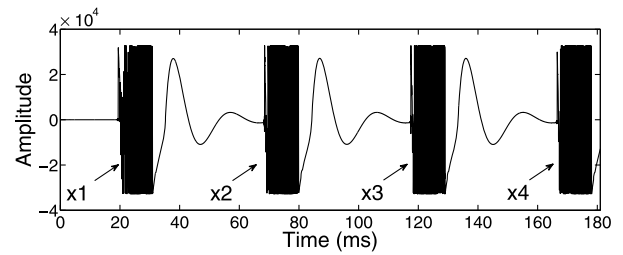


Fig. 6. 8000 samples obtained from a single reading of the buffer.

Fig. 5 shows a circuit schematic of the modulator. The modulator is designed to turn the carrier frequency ON and OFF. Once the pulse-width modulated signal goes high, the transistor saturates, and the carrier is transferred to the phone. Once the pulse-width signal goes low, the transistor enters cut-off mode, and the carrier is truncated. By switching the carrier frequency ON and OFF as the pulse transitions from low-to-high and high-to-low, it is possible to generate an ac signal that has approximately the same length as the pulse width modulated signal.

### B. Demodulation

The external module continuously and asynchronously transmits distance readings to the phone, where they get stored in the phone’s audio buffer. An application running on the phone reads from this buffer in chunks of 8000 samples (equivalent to about 181 ms at a 44.1-kHz sample rate).

Since the external module is generating readings every 50 ms, it is possible to have at most approximately three signals in each chunk that have not been truncated. Fig. 6 shows a plot of the values from the signal buffer. The signals  $x_1$ ,  $x_2$ ,  $x_3$ , and  $x_4$  represent four different readings. Notice that signal  $x_4$  is truncated because of the buffer size, and therefore its length does not reflect the correct measurement, so it must be discarded. For a more complicated design, a producer consumer design pattern can be used to create a continuous buffer. In the ideal case, the remaining signals,  $x_1$ ,  $x_2$ , and  $x_3$  would be the same length. However, we see a stabilization error in the digital signal when we try to decode it. Since the smartphone’s hardware is proprietary, we cannot easily tell exactly what is causing the transient response, but we think it may be due to ac coupling, since the direct current (dc) bias is removed in the

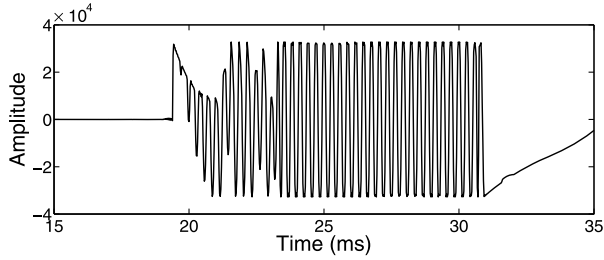


Fig. 7. Single reading from the buffer, i.e.,  $x_1$  from Fig. 6.

received signal. Fig. 7 shows a zoomed in section of one of the signals that has been reconstructed on the phone. Notice that it takes approximately 4 ms for the signal to stabilize, from the 31 ms mark to 35 ms. This may be due to the transient response of the pulse-width component that is still present in the signal. However, it is possible to mitigate this during the demodulation process. Since, the first and last peaks are always reconstructed correctly, and the frequency of the carrier is known, the number of peaks in the signal can be calculated using the, known, time between the first peak and the last peak. This approach removes any errors that are introduced by peaks that are not correctly reconstructed in the signal.

1) *Demodulation Algorithm*: Once the signal has been modulated by the external attachment, it needs to be demodulated by the software on the smartphone, so that the signal can be converted back to a distance reading. To handle this decoding process, we use a linear time demodulation algorithm. The algorithm works by counting the number of peaks that are above a particular threshold. Recall that the frequency of the carrier was selected carefully, so that each peak corresponds to 2 inches (0.051 m). The threshold is automatically selected by the software to be 50% of the maximum value in the buffer. Having the software automatically select the threshold will help mitigate the differences in the sound interfaces on different devices.

### C. 2-D Map Generation

Since we collect information on both the distance and direction of an object from the phone, we can generate a 2-D map of a space by taking multiple measurements in different directions. Recall that the phone's orientation can be determined by using its internal magnetometer, gyroscope, and accelerometer. We map a room by rotating the phone through a single 360° rotation. As a convention, we define 0° to be north and values increase in a clockwise direction (e.g., east is 90°). Since the magnetometer is noisy, the direction values are discretized into 20° increments [9], [13]. The application divides the compass into 18 sections of 20°. A measurement taken in a given section will associate that value with the center of that section. We can then generate a relatively stable measurement by using the values of the phone's pitch to help compensate for the phone orientation.

We implemented the design on a Nexus 4 smartphone. Fig. 8 shows a screenshot of the application. The application shows the distance, pitch, and direction values, as well as a polar plot generated from a collection of measurements.

### Algorithm 1. Calculate signal width

**Input:** array, threshold

**Output:** PeakArray

first = true; firstIndex = 0; lastIndex = 0; for  $i = 0$ ;

$i < \text{array.length}$ ;  $i++$  do

if  $\text{array}[i] > \text{array}[i - 1]$  and  $\text{array}[i] > \text{array}[i + 1]$   
||  $\text{array}[i] < \text{array}[i - 1]$  and  $\text{array}[i] < \text{array}[i + 1]$   
then

if  $\text{array}[i] \geq \text{threshold}$  ||  $\text{array}[i] \leq -\text{threshold}$   
then

peakSeen = true;  
count++;

if first then

firstIndex =  $i$ ;

first = false;

end

else

lastIndex =  $i$ ;

end

end

if peakSeen then

hops++;

end

if hopExpire < hops then

if count > 2 then

distances.add(lastIndex - firstIndex);

end

hops = 0;

count = 0;

peakSeen = false;

first = true; firstIndex = 0; lastIndex = 0;

end

end

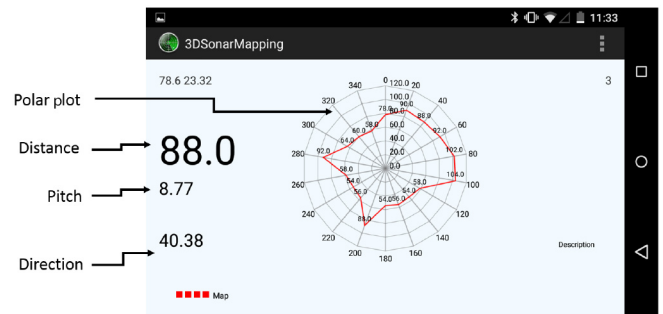


Fig. 8. Screenshot of the mapping application showing the information on distance (in inches), direction (in degrees, with 0° at north), pitch (in degrees, with 0° at horizontal, i.e., to the ground), and the resulting polar plot.

### D. Possible Applications

Now that we have shown that it is possible to do depth sensing using SONAR on smartphones, the question naturally arises: “What can this be used for?” We have several ideas for possible applications of depth sensing using SONAR. The system may be used to create a SONAR cane that allows people with visual impairments to navigate a space. The system

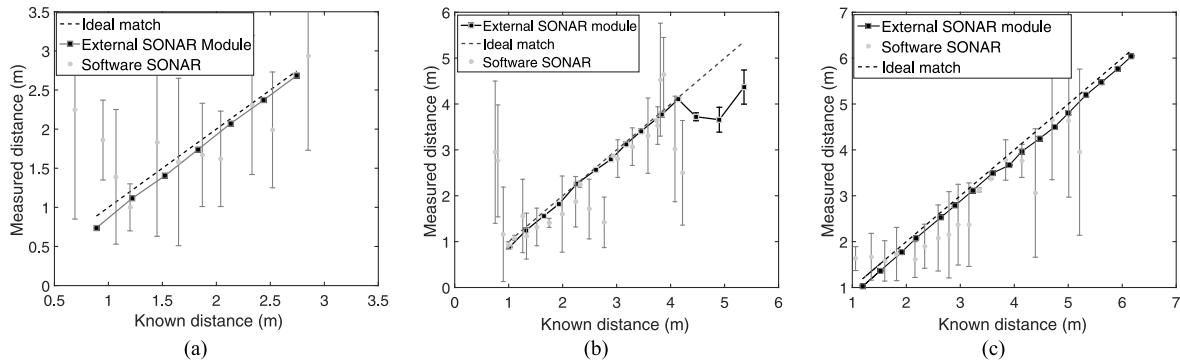


Fig. 9. (a) Small room  $A_s = 0.42$ ,  $A_h = 0.09$ . (b) Large room  $A_s = 0.22$ ,  $A_h = 0.07$ . (c) Noisy outside area  $A_s = 0.38$ ,  $A_h = 0.16$ . Ten measurements were taken at each distance; the error bars represent the standard deviation of these measurements.  $A_s$  represents the average error for software SONAR module and  $A_h$  the average error for the software module.

can also be used as a tool for realtors, interior designers, or engineers to quickly get an estimate of the dimensions of the room.

### III. EVALUATION

We evaluated our system using two metrics, accuracy, and spatial resolution, in a small room, a large room, and an outdoor environment. In measuring the external SONAR attachment's accuracy, we compared it to our previous software-based SONAR sensor [6] and a commercial sonar measuring device called the Strait-Line Laser Tape [4]. The external attachment achieved much lower standard deviations at each measured distance and smaller error when compared to the software-based SONAR from our previous work.

In evaluating the spatial resolution, we took a collection of measurements in different directions to generate a polar plot of the area around the phone (as described in Section II-C), and compared the plot to the actual floorplan of the room.

#### A. Evaluating Accuracy

We evaluated the accuracy of our external SONAR by placing it on a tripod and taking measurements at different distances in three environments (for all tests we used the Nexus 4). At each distance, ten measurements were taken using both the external SONAR module and the software-based SONAR module. The average value and standard deviation of these readings were plotted against the actual distance for all three environments. The average error for both the external module  $A_h$  and the software-based SONAR application  $A_s$  were calculated, excluding the break down regions (i.e., less than 1 m and more than 4 m for the software SONAR, and less than 0.5 m for the external sonar module).

The first environment was a small room (approximately  $3.36 \times 3.92$  m). Fig. 9(a) shows the results of this experiment. For the software SONAR sensor, we see decreased performance at values lower than 1 m. When we compare the result of the values obtained using the external SONAR attachment, we noticed that the values have a much smaller standard deviation and are more accurate. The smaller beam of sound

that is produced from the external sensor helps mitigate the reverberation effects.

The second environment was a large carpeted indoor room (approximately  $8.61 \times 6.10$  m). Fig. 9(b) shows the results of this experiment. The software-based SONAR module performs much better in a large indoor room but begins to break down after 3.5 m. As for the attachment, as the distance increases, so does the beam width. At 5.5 m, the beam is wide enough to pick up other objects in the space, like desks and chairs. This causes the accuracy of the sonar sensor to decrease as distance from the wall increases.

The final environment was an outdoor area with moderate building construction noise in the background. Fig. 9(c) shows the results of this experiment. From these results, we can see that the external SONAR module outperforms the software-based sensor. Even though external module does sometimes underestimate the distance, it continued to perform up to its design limit of approximately 6 m. This design limit is determined by the maximum distance of the transducer module which, from the datasheet, we know is approximately 20 ft, or 6.1 m. Though it is possible to increase the system's range by purchasing a new transducer module; such modules are normally much larger and have a large cone that surrounds the buzzer. In an effort to maintain a small, convenient form factor, we have opted to not use a smaller transducer module.

#### B. Evaluating Resolution

In this section, we evaluate the spatial resolution of the system by generating a 2-D map of a space and displaying it on a polar plot. Fig. 10(a) shows a polar plot that was obtained by placing the smartphone on a tripod in the middle of the small room and rotating it  $360^\circ$ . We then measured the room, using a compass to determine the room's orientation, and calculated its polar coordinates. These values were then overlaid on the measured values in Fig. 10(a). We repeated this process for the other two environments and plotted in the results in Fig. 10(b) and (c).

#### C. Sources of Error

There are two main sources of noise when generating polar plots. The first source is noise from the gyroscope and

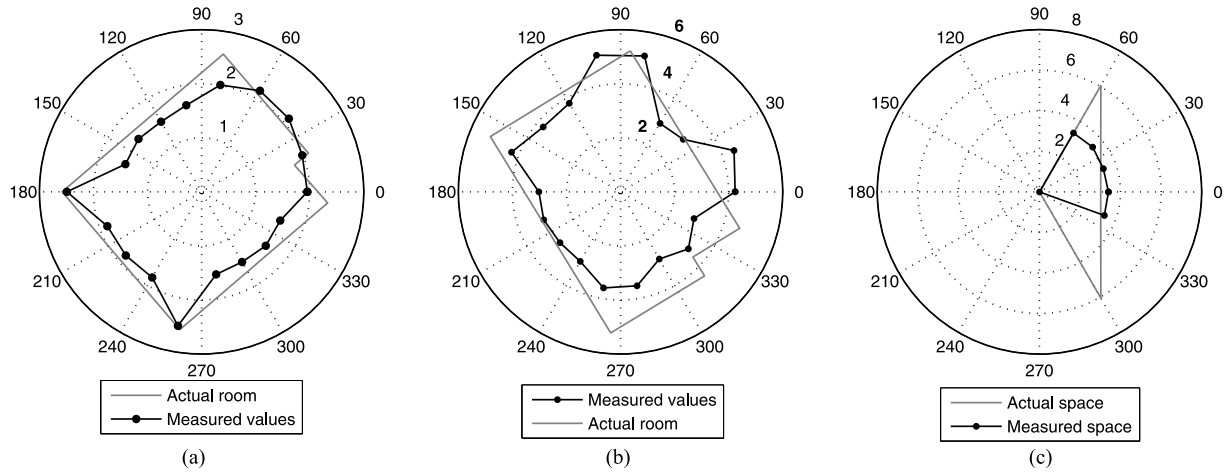


Fig. 10. Polar values obtained by the external SONAR module in (a) small room, (b) large room, and (c) outdoor environment. The application divides the compass into 18  $20^\circ$  sections. A measurement taken in a given section will associate that value with the center of that section. All measurements shows are in meters and all angles are in degrees.

magnetometer. The magnetometer determines the smartphone's direction with respect to magnetic north by sensing the earth's magnetic field. However, the magnetometer is noisy and sometimes the direction is not determined correctly. We believe that this is the reason for the distorted corners in the large room measurement. The other source of error may be due to the fact that surfaces reflect sound at an angle to the surface normal. This means that the system will be fairly accurate when taking measurements of an object that is directly in front, but as the angle from the receiver to the object increases, the accuracy will decrease, since less energy is being reflected in the direction of the receiver.

#### D. Energy Consumption

Another unique aspect of our design is that it is internally powered and does not require power from the phone. The only energy that is consumed by the phone is the energy that is associated with processing the information that is generated by the sensor. Since there are several other processes on the phone, it is difficult to isolate the energy that is consumed by only the demodulation process. The notion of harvesting energy from the phone to power the external sensor is interesting, though we do not do it for this sensor, other researchers and engineers have adopted this approach. For example, the highjack prototype developed by researchers at the University of Michigan uses energy harvesting [8]. However, we did not opt for this approach due to the additional complexity associated with implementing it. Implementing this energy harvesting approach would include the addition of a bridge rectifier to convert the ac signal to dc signal, and a voltage multiplier to step up the signal to the required voltage.

#### E. Testing Other Devices

So far throughout our evaluation, we have only used the Nexus 4. But the question remains, Will this solution generalize to other devices? In an effort to answer this question, we evaluated our interface design on six different devices. The results of

TABLE I  
COMPATIBLE DEVICES

Device	OS	Mismatch	App worked	App failed
LG Nexus 4	5.1.1	✓	✓	
Samsung 5	4.4.2			✓
Samsung 4	4.4.4			✓
Nexus 5	5.1.1 & 4.4.3	✓		✓
LG L90	4.4.4	✓		✓
LG MyTouch QC 800	4.0.1	✓	✓	

these tests are summarized in Table I. We found that the interface mismatch issue existed on four of the six devices that we tested. We also tested the mapping application on these devices, and found that the application worked on two of the six devices that we tested. We are currently searching for the hardware or software issues that may have caused the failures in these other devices. One possible source of failure may be due to the operating system automatically lowering the volume when the headphone jack is plugged in. This makes it difficult to get a strong enough carrier for the modulator. Future versions of the hardware may need to include an amplifier and buffer on the interface board.

#### F. Testing in an Irregular Environment

So far we have tested the external attachment in simple environments. In this section, we evaluate the performance of the system in a stairwell. Fig. 11 shows a photograph of the stairwell and Fig. 12 shows the results of the map that was generated. From the figure, we notice that errors from the magnetometer cause the map to be slightly skewed, e.g., in Fig. 12, the points at  $100^\circ$  and  $260^\circ$ . We also notice that sensor picks up the middle of the staircase that is blocking the rear wall. We can also see that sensor does not pick up the lower rear wall due to the narrow beam width. All of these factors along with the irregular nature of the stairwell result in a moderate reconstruction of the space.



Fig. 11. Photograph of the stairwell in which the measurements were taken.

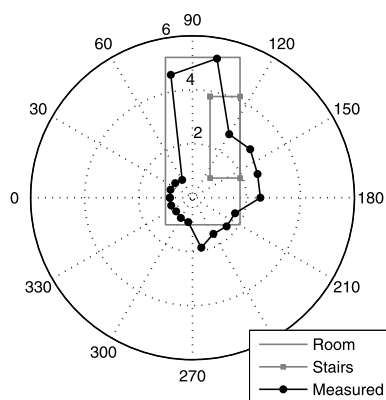


Fig. 12. Map that was reconstructed from the measurements taken in the stairwell. All measurements are in meters and directions are in degrees.

#### IV. RELATED WORK

In 2010, researchers at the University of Michigan explored a way of connecting external devices to smartphones via the headphone jack, called *hijack* [8]. A unique aspect of their design was that they harvested energy from the headphone jack to power the microcontroller which was responsible for processing sensor data and performing modulation tasks. They also proposed using a frequency shift key encoding scheme to communicate with the phone over the headphone jack, where it was demodulated using software installed on the phone. Several external mobile attachments have been developed using the *hijack* platform [7], [11], [14]. However, it is also possible to design a modulator that does not require the use of a processor. Such a modulator would provide the software application on the phone with control of carrier frequency and with it, the baud rate. The modulator in this paper uses a hybrid hardware/software approach to modulate the signal and does not require the use of a microcontroller. Since the modulator design does not include a microcontroller, there is also no need to implement any firmware. The proposed hybrid hardware/software modulator is comprised of a collection of simple analog components which are used to modulate a carrier supplied by the smartphone.

Project tango, by Google's advance technology and applications group, integrates a 3-D depth sensing camera into a smartphone, hereby providing the smartphone with the ability to generate 3-D maps of space [3]. The inclusion of this sensor in smartphones has opened a collection of new accessibility

applications, including indoor navigation and obstacle detection. Developing depth sensing sensors for smartphones will help advance the field of assistive technologies. Researchers have also explored ways of providing depth sensing capabilities without the use of specialized hardware, instead choosing to implement software-based SONAR ranging sensor solutions [6]. These sensors use a collection of chirps to determine the distance from the sensor to an object in space. However, these software-based sensors are limited by the hardware constraints of the phone, since microphones and speakers are located at different locations on different phones. Creating external sensors will help mitigate this constraint and facilitate the development of assistive technologies such as SONAR canes. Though SONAR-based navigation devices such as SONAR canes [5] already exist, providing attachments for devices that are already carried by the visually impaired will replace custom embedded solutions.

#### V. CONCLUSION

In this paper, we proposed a design for a smartphone compatible external SONAR module as an extension on our previous research into software-based SONAR sensors for smartphones [6].

We designed a hybrid hardware/software modulator that allows the external attachment to communicate with the phone via the headphone jack. The modulator design is unique because it does not use a hardware oscillator to generate the carrier frequency but instead uses the software on the phone and the phone's DAC. The modulator encodes the range information from the external module using a modulated continuous carrier. This information is then decoded and combined with information from the phone's gyroscope, accelerometer, and magnetometer to generate a 2-D map of the space.

A possible avenue for future research is exploring ways of improving the hybrid modulator, by using a photo relay as a switch instead of transistor. This would mitigate the stabilization time in the buffer signal by potentially eliminating the dc bias from the transient response of the pulse-width component.

#### REFERENCES

- [1] Honeywell. "Captuvo s142 enterprise sled for Apple iPhone 5th generation," [Online]. Available: <https://www.honeywellaidc.com/en-US/Pages/Product.aspx?category=enterprise-sleds-for-apple-devices&cat=HSM&pid=captuvosl42v5>, accessed on Jun. 14, 2015.
- [2] Maxbotix. "Lv-maxsonar-ez series," [Online]. Available: [http://maxbotix.com/documents/LV-MaxSonar-EZ\\_Datasheet.pdf](http://maxbotix.com/documents/LV-MaxSonar-EZ_Datasheet.pdf), accessed on Jun. 23, 2015.
- [3] Google. "Project Tango," [Online]. Available: <https://www.google.com/atap/project-tango/about-project-tango/>, accessed on Jun. 15, 2015.
- [4] Irwin Tools. "Strait-line," [Online]. Available: [http://www.irwin.com/uploads/documents/36\\_laser\\_tape\\_25.pdf](http://www.irwin.com/uploads/documents/36_laser_tape_25.pdf), accessed on Jun. 23, 2015.
- [5] R. Farcy, R. Leroux, A. Jucha, R. Damaschini, C. Grégoire, and A. Zogaghi, "Electronic travel aids and electronic orientation aids for blind people: Technical, rehabilitation and everyday life points of view," in *Proc. Conf. Workshop Assist. Technol. People Vis. Hear. Impair. Technol. Inclusion*, 2006, p. 12.
- [6] D. Graham, G. Simmons, D. Nguyen, and G. Zhou, "A software based sonar ranging sensor for smart phones," *IEEE Internet Things J.*, vol. 2, no. 6, pp. 479–489, Dec. 2015.

- [7] D. Hong *et al.*, "Demo abstract: Septimucontinuous in-situ human wellness monitoring and feedback using sensors embedded in earphones," in *Proc. ACM/IEEE 11th Int. Conf. Inf. Process. Sens. Netw. (IPSN)*, 2012, pp. 159–160.
- [8] Y.-S. Kuo, S. Verma, T. Schmid, and P. Dutta, "Hijacking power and bandwidth from the mobile phone's audio interface," in *Proc. 1st ACM Symp. Comput. Dev.*, 2010, p. 24.
- [9] J. A. B. Link, P. Smith, N. Viol, and K. Wehrle, "Footpath: Accurate map-based indoor navigation using smartphones," in *Proc. Int. Conf. Indoor Position. Indoor Navig. (IPIN)*, 2011, pp. 1–8.
- [10] A. Molnar, B. Lu, S. Lanzisera, B. W. Cook, and K. S. Pister, "An ultra-low power 900 MHz RF transceiver for wireless sensor networks," in *Proc. IEEE Custom Integr. Circuits Conf.*, 2004, pp. 401–404.
- [11] S. Nirjon *et al.*, "Musicalheart: A hearty way of listening to music," in *Proc. 10th ACM Conf. Embedded Netw. Sens. Syst.*, 2012, pp. 43–56.
- [12] J. G. Proakis, M. Salehi, N. Zhou, and X. Li, *Communication Systems Engineering*. Englewood Cliffs, NJ, USA: Prentice-Hall, 1994, vol. 1.
- [13] H. Shin, Y. Chon, and H. Cha, "Unsupervised construction of an indoor floor plan using a smartphone," *IEEE Trans. Syst. Man Cybern. C, Appl. Rev.*, vol. 42, no. 6, pp. 889–898, Nov. 2012.
- [14] S. Verma, A. Robinson, and P. Dutta, "Audiodaq: Turning the mobile phone's ubiquitous headset port into a universal data acquisition interface," in *Proc. 10th ACM Conf. Embedded Netw. Sensor Syst.*, 2012 pp. 197–210.



**Daniel Graham** received the B.S. degree and M.Eng. degree in systems engineering from the University of Virginia, Charlottesville, VA, USA, in 2010 and 2011, respectively, and is currently working toward the Ph.D. degree in computer science at the College of William and Mary, Williamsburg, VA, USA.

His research interests include intelligent embedded systems and networks.



**Gang Zhou** received the Ph.D. degree from the University of Virginia, Charlottesville, VA, USA, in 2007.

He is currently an Associate Professor with the Department of Computer Science, College of William and Mary, Williamsburg, VA, USA. He has authored over 70 academic papers in the areas of ubiquitous computing, mobile computing, sensor networks, and wireless networks.

Dr. Zhou is a Senior Member of ACM. He is currently serving on the Editorial Board of the IEEE INTERNET OF THINGS JOURNAL, as well as Elsevier's *Computer Networks*. He was the recipient of an award for his outstanding service to the IEEE Instrumentation and Measurement Society in 2008. He was the recipient of the Best Paper Award of the IEEE ICNP 2010 and NSF CAREER Award in 2013.



**Ed Novak** received the B.A. degree from Monmouth College, Monmouth, IL, USA, in 2010, the M.S. degree in computer science from the College of William and Mary, Williamsburg, VA, USA, in 2012, and is currently working toward the Ph.D. degree in computer science at the College of William and Mary.

His research interests include privacy and security on mobile devices and wearable computing.



**Jeffrey Buffkin** is currently working toward the B.S. degree in physics and mathematics at the College of William and Mary, Williamsburg, VA, USA.

He has performed research with Q-weak, which utilized a J-Lab particle accelerator to find an experimental value for the weak charge of quarks through parity-violating electron scattering. His research interests include electronics and embedded systems.